Appl Phys B (2010) 101: 587–591
DOI 10.1007/s00340-010-4237-x

**Applied Physics B**
**Lasers and Optics**

# Compression grating alignment by far-field monitoring

**F. Liu · X.L. Liu · Z.H. Wang · J.L. Ma · X. Liu · L. Zhang · J. Wang · S.J. Wang · X.X. Lin · Y.T. Li · L.M. Chen · Z.Y. Wei · J. Zhang**

Received: 18 October 2009 / Revised version: 16 August 2010 / Published online: 5 November 2010


**Abstract** Slight non-parallelism of the gratings in the compressor of a chirped-pulse amplification laser system produces angular chirp which results in a significant reduction of the focused intensity due to elongation of the pulse duration and enlargement of the focal spot. The effect of three-dimensional relative misalignment angles between two gratings on the far-field pattern of the pulses propagating through them is investigated by ray tracing. The far-field pattern provides two-dimensional information of the uncompensated angular dispersion directly. A simple and intuitive alignment procedure to achieve parallelism of the compression gratings by far-field monitoring is demonstrated experimentally, while the alignment precision is found to be the same as the methods proposed previously.

## 1 Introduction

Recent continuous developments of ultra-short intense laser systems using the technology of chirped-pulse amplification (CPA) [1] make it possible to construct table-top laser facilities delivering pulses with peak power of PW [2] and focused intensity of $10^{22}$ W/cm$^2$ [3]. Ultra-short seed pulses are stretched temporally by going through a dispersive optical element such as a fiber [4] or grating [5, 6] based stretcher. After amplification, the pulses are recompressed to the original pulse duration by an opposite dispersive device such as grating pair [7]. It is crucial to align the grating pair in the compressor precisely to prevent spatial and temporal distortions. Slight non-parallelism of the grating pair introduces angular chirp which results in a pulse-front tilt in the near field [8, 9]. When the laser pulse with angular chirp is focused, the intensity in the focal plane will be significantly reduced due to elongation of the pulse duration and enlargement of the focal spot [10].

In order to measure the angular chirp and accurately align the parallelism of the compression gratings in CPA laser systems, several diagnostic devices have been developed, including interferometric field autocorrelation [10], tilt pulse-front single-shot autocorrelation [11], imaging spectrography [12], spectrally resolved interference [13], and single-shot second-harmonic-generation frequency-resolved optical gating (SHG FROG) measurements [14]. Interferometric field autocorrelation does not work in real time because it requires multi-shot operation. Tilt pulse-front single-shot autocorrelation can monitor the pulse-front tilt and duration simultaneously, but it needs high-intensity pulses for second-harmonic generation. Moreover, all of these methods make the setup complex and can only detect the angular chirp in one dimension. The usual compressor alignment procedure [15] is straightforward but not accurate enough. Two individual alignment lasers with different wavelengths are used to align the compression gratings precisely in a Nd:glass laser system [16]. However, it is difficult to obtain alignment lasers with wavelengths covering the whole spectral width of the pulses generated in a Ti:sapphire laser

F. Liu · X.L. Liu · Z.H. Wang · J.L. Ma · X. Liu · L. Zhang · J. Wang · S.J. Wang · X.X. Lin · Y.T. Li · L.M. Chen · Z.Y. Wei · J. Zhang (✉)
Beijing National Laboratory for Condensed Matter Physics, Institute of Physics, Chinese Academy of Sciences, Beijing 100190, P.R. China
e-mail: jzhang@aphy.iphy.ac.cn
Fax: +86-10-82649356

J. Wang
Institute of Physics, Nankai University, Tianjin 300071, P.R. China

J. Zhang
Department of Physics, Shanghai Jiao Tong University, Shanghai 200240, P.R. China

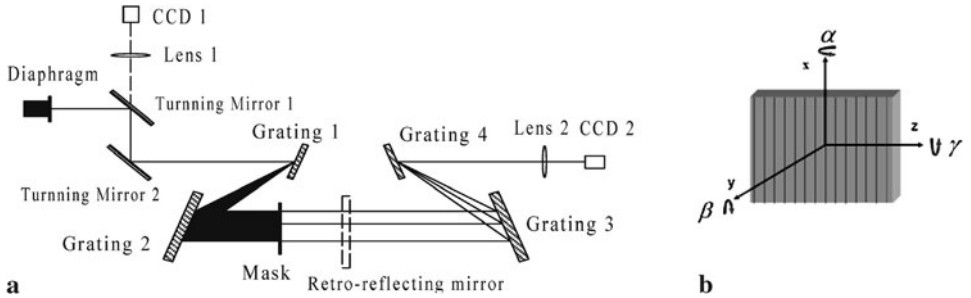


**Fig. 1** (**a**) Sketch of a four-grating compressor (*top view*). The laser pulses are injected into the compressor from the left and exit it on the right. *Lens 1*, *CCD 1*, *retro-reflecting mirror*, *lens 2*, and *CCD 2* are used in the experiment to monitor the far-field pattern of a beam after a double pass of *gratings 1* and *2* and a single pass of the four-grating compressor, respectively. (**b**) Definition of the rotation angles $\alpha$, $\beta$, and $\gamma$ around the $x$-, $y$-, and $z$-axes of the grating relative to its perfectly aligned orientation

system. The wavelength differences between the alignment lasers and the high-power laser as well as the overlapping mismatch between the alignment lasers will introduce additional alignment errors.

In this paper, we present a very simple method to assure the parallelism of the compression gratings. The laser beam is angularly dispersed by the first grating and collimated by the second grating. A mask downstream of the second grating is used to select several narrow-band spectral components from the beam, and the output beam is focused onto a CCD (charge-coupled-device) camera. The compression gratings are accurately aligned by monitoring the two-dimensional beam profile in the focal plane.

## 2 ZEMAX ray tracing

We performed ray tracing using the commercial optical design software ZEMAX to study the influence of a misaligned grating pair on the far-field pattern of a beam propagating through it. Figure 1a shows a sketch of a single-pass four-grating compressor which is equivalent to a double-pass grating pair compressor with a retro-reflecting mirror. We define the rotation angles $\alpha$, $\beta$, and $\gamma$ around the $x$-, $y$-, and $z$-axes of a grating relative to its perfectly aligned orientation as indicated in Fig. 1b. The dimensions of gratings 1 and 4 are 230 mm $\times$ 180 mm $\times$ 30 mm, and those of gratings 2 and 3 are 460 mm $\times$ 210 mm $\times$ 50 mm. The groove densities of the four gratings are equal and amount to 1480 lines/mm. A laser beam of 100-mm diameter hits the first grating under the incidence angle of 20.5° and then propagates through the compressor. Seven wavelengths in the range from 770 nm to 830 nm with an interval of 10 nm are used in the ray tracing. The output beam is focused by a 1000-mm focal length lens. The spatial profiles of the laser beam in the focal plane are investigated.

The focal spots when grating 4 deviates slightly from its perfectly aligned orientation are shown in Fig. 2. The rotation of the grating around the $x$-axis ($\alpha = 1$ mrad) elongates the focal spot horizontally in the diffraction plane as shown in Fig. 2a. The rotation of the grating around the $z$-axis ($\gamma = 1$ mrad) elongates the focal spot vertically in the plane perpendicular to the diffraction plane as shown in Fig. 2b. The effect of rotation of the grating grooves around the $y$-axis is similar. When the grating surface has deviations around the $x$-axis and the $y$-axis simultaneously ($\alpha = 1$ mrad, $\gamma = 1$ mrad), a tilted and elongated focal spot will be observed as shown in Fig. 2c. When the rotation of the grating grooves around the $y$-axis is added further ($\alpha = 1$ mrad, $\beta = 1$ mrad, $\gamma = 1$ mrad), the different spectral components will no longer be in a line but curved as presented in Fig. 2d. It is worth mentioning that this phenomenon can be used as a criterion of whether there are alignment errors due to both grating surface rotation around the $z$-axis and groove rotation around the $y$-axis, which cannot be determined easily by other techniques using only one-dimensional diagnostics [10–14] or two wavelengths [16].

## 3 Experimental results and discussion

We discuss how to achieve the parallelism of the compression gratings step by step. The gratings are installed in the geometrical position and pre-aligned using the usual method [15]. The pulses delivered by the oscillator are expanded to about 100-mm beam diameter and then injected into the compressor at the designed incidence angle of 20.5° onto the first grating. After propagation through the compressor, the pulses are focused onto a CCD camera to view the far-field pattern.

First of all, it is needed to distinguish the focal spot distortion induced by angular chirp introduced by grating misalignment from other sources such as aberrations caused by poor-quality optics. The focal spot of the laser beam when the oscillator is in continuous-wave operation is compared to that when the oscillator is in mode-locked operation. As shown in Fig. 3a, the focal spot of the mode-locked pulses is

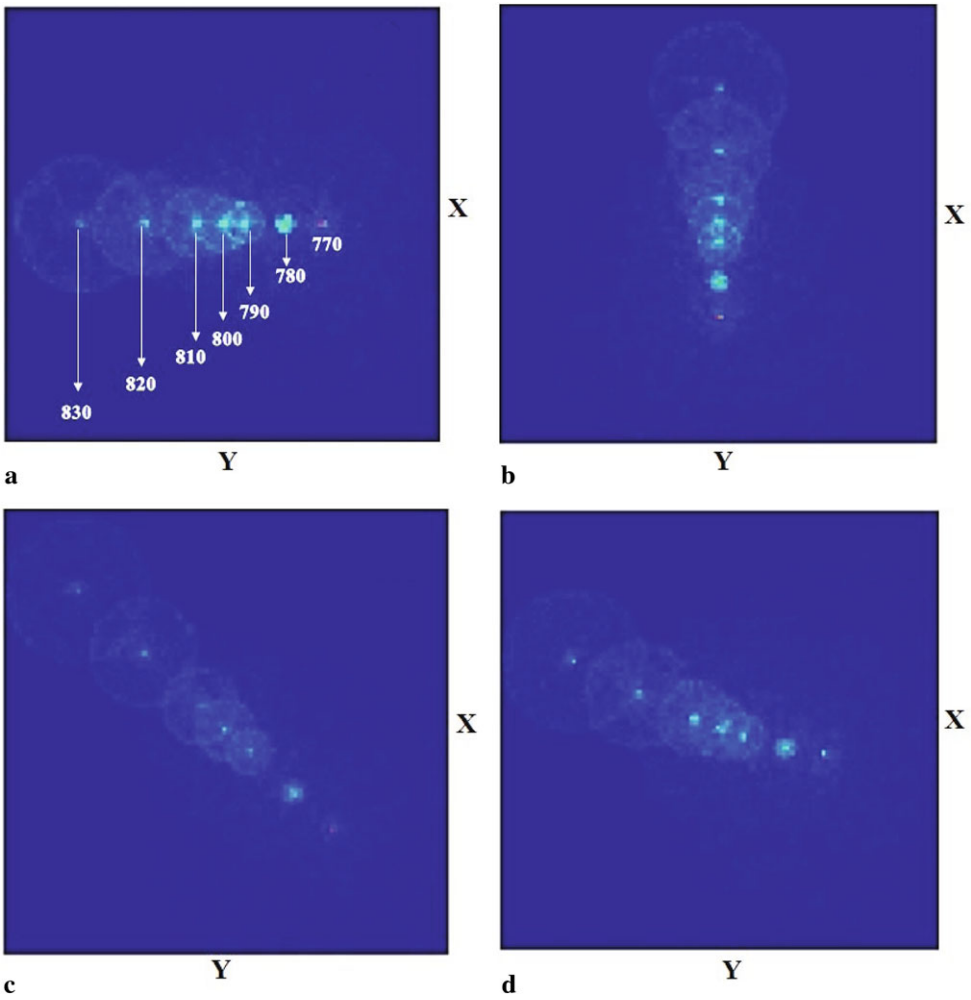


**Fig. 2** Patterns of the output beam in the focal plane when grating 4 has a small-angle deviation from its perfectly aligned orientation: (**a**) $\alpha = 1$ mrad, (**b**) $\gamma = 1$ mrad, (**c**) $\alpha = 1$ mrad and $\gamma = 1$ mrad, (**d**) $\alpha = 1$ mrad, $\beta = 1$ mrad, and $\gamma = 1$ mrad. The image dimension is 500 μm × 500 μm. The spots corresponding to different wavelengths as indicated in (**a**) are due to spectral decomposition in the focal plane

dramatically elongated and tilted while the continuous wave is almost perfectly focused. Because all the other parameters are exactly the same in the two cases except for the spectral width, the exclusive cause of the degradation of the focal spot is the angular chirp introduced by the diffractive optical elements in the system—the gratings.

The parallelism of the first grating pair is aligned by adjusting grating 2 while grating 1 is fixed. As shown in Fig. 1a, a diaphragm with an aperture diameter of about 10 mm is installed in the beam path to get a small-sized beam. After the beam is diffracted by grating 1 and collimated by grating 2, a mask with holes is used to select several narrow-band spectral components from the beam. All of these spectral components are picked up from the same oscillator beam, so they are inherently collinear before entering the compressor and cover the whole spectral width of the high-power amplified pulses. This is similar to the method used in [16], but much more convenient and easy for alignment. A retro-reflecting mirror reflects the laser beam back into the incoming beam path to double pass the grating pair. The retro-reflected beam leaking through turning mirror 1 is focused by lens 1 onto CCD camera 1.

The decomposition of the different spectral components into different directions can be observed in the focal plane. The spots of individual spectral components will be curved as illustrated in Fig. 2d when there are three-dimensional alignment errors between gratings 1 and 2. First, the groove orientation can be adjusted by rotation of grating 2 around the $y$-axis until the spots are in a line as shown in Fig. 3b. Second, the surface vertical orientation can be adjusted by rotating grating 2 around the $z$-axis until the spots are in a horizontal line as shown in Fig. 3c. Third, the surface horizontal orientation can be adjusted by rotating grating 2 around the $x$-axis until all spectral components merge into one spot as shown in Fig. 3d. The parallelism of the second grating pair is aligned following the same procedure by monitoring the far field of the output beam from grating 4 using lens 2 and CCD camera 2. The delicate adjustment of the two grating pairs is finished by verifying that the far-field pattern of the mode-locked pulses leaving the compressor is the same as that of the continuous wave as presented in Fig. 3e. Finally, only the distance between the gratings needs to be adjusted when the amplified pulses are injected

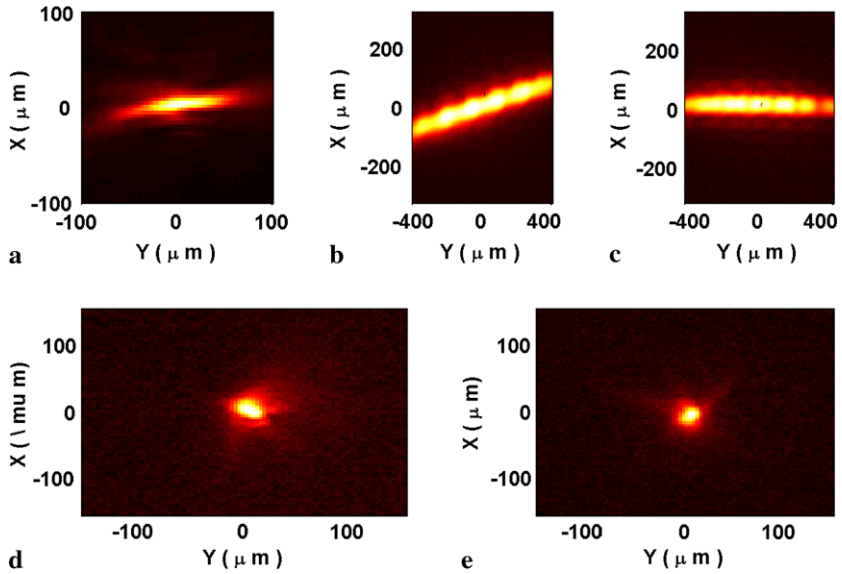


**Fig. 3** Example of compression grating parallelism alignment procedure by far-field monitoring: (**a**) focal spot obtained after the gratings have been pre-aligned by the usual method. The focal spot is dramatically elongated and tilted. (**b**) Adjust the groove rotation around the $y$-axis until the focal spots formed by different spectral components are in a line instead of a curve. (**c**) Adjust the surface rotation around the $z$-axis until the focal spots are in a horizontal line. (**d**) The far-field pattern of a beam after a double pass of gratings 1 and 2 which are well aligned and (**e**) the far-field pattern of a beam after a single pass of a well-aligned four-grating compressor

into the compressor to obtain minimal pulse duration after compression.

Now, we analyze the alignment error of our proposed method. Grating 2 is assumed to have a misalignment in the dispersion plane due to a slight angle $\alpha$ around the $x$-axis. The laser beam will have uncompensated angular dispersion after propagation through the non-parallel grating pair. The angular difference between wavelengths $\lambda_1$ and $\lambda_2$ is given by $\delta\varphi = \alpha(\cos\theta_1 - \cos\theta_2)/\cos\theta_i$, where $\theta_1$ and $\theta_2$ are the diffraction angles corresponding to wavelengths $\lambda_1$ and $\lambda_2$, respectively [10]. The double pass of the beam through the grating pair will double the angular difference. When the output beam is focused, the angular chirp will result in a decomposition of different spectral components in the focal plane as shown in Fig. 3c. The displacement between the focal spots is given by $\delta y = f2\delta\varphi$, where $f = 500$ mm is the focal length of the lens. The displacement should be less than half of the focal spot diameter of $D = 20$ μm as shown in Fig. 3d. So, we obtain $f2\delta\varphi < 1/2D$, which results in $\alpha < D\cos\theta_i/(4f(\cos\theta_1 - \cos\theta_2))$. The spectrum of the laser beam from our oscillator ranges from 750 nm to 850 nm, so we estimate the alignment error to be $\alpha < 40$ μrad. Using the formulas given in [10], the alignment errors in the other two orientations are estimated to be $\beta < 67$ μrad and $\gamma < 44$ μrad, respectively.

As analyzed above, the maximum alignment error limit of our suggested procedure is reached when the focal spot of the mode-locked pulses elongates to half of that of the continuous wave. For the inverted field autocorrelation measurement, the angular chirp is measured by the variation of the interference contrast [10]. The maximum alignment error limit is reached when the group delay across the beam introduced by the residual angular chirp is less than the coherence time, which is equal to the Fourier-transform-limited pulse duration. There is the same situation for the FROG measurement where the angular chirp is measured by the displacement of the FROG trace center [14]. Again, the maximum alignment error limit is reached when the group delay across the beam is equal to half of the pulse duration. Angular chirp leads to the focal spot and pulse duration being enlarged by the same factor [10]. So, theoretically, all of these proposed methods have the same maximum alignment error inherently limited by the spectral width or Fourier-transform-limited pulse duration.

Finally, if we take into account the fact that the spectral width of the pulses for alignment delivered by the oscillator is much larger than that of the amplified pulses due to gain narrowing during amplification (the spectral width of the pulses from the oscillator is larger than 100 nm, while that of the amplified pulses is less than 50 nm in our case), we think that the alignment precision is good enough and the influence of the residual angular chirp on the focused intensity is negligible.

## 4 Conclusion

The influence of the relative misalignment angles between the gratings on the far-field pattern of the output beam was

investigated by ray tracing. Slight non-parallelism of the grating pair introduces angular chirp which results in significant distortions of the focal spot. It is demonstrated that the compression gratings can be accurately aligned by real-time monitoring of the far-field pattern of the output beam. The alignment error is limited by the fact that the focal spot is not significantly distorted by the uncompensated angular dispersion introduced by the non-parallel grating pair. The maximum alignment error of our proposed procedure is found to be the same as the methods proposed previously. In order to obtain enough alignment precision, the solution is to use alignment laser sources with spectral width larger than that of the amplified pulses to be compressed.

**Acknowledgements** The authors would like to thank Prof. Klaus J. Witte for helpful discussions and improving the manuscript. This work is supported by the National Natural Science Foundation of China (Grant Nos. 60621063 and 10925421) and the National Basic Research Program of China (973 Program) (Grant No. 2007CB815101).

## References

1. D. Strickland, G. Mourou, Opt. Commun. **56**, 219 (1985)
2. M. Aoyama, K. Yamakawa, Y. Akahane, J. Ma, N. Inoue, H. Ueda, H. Kiriyama, Opt. Lett. **28**, 1594 (2003)
3. S.-W. Bahk, P. Rousseau, T. Planchon, V. Chvykov, G. Kalintchenko, A. Maksimchuk, G. Mourou, V. Yanovsky, Opt. Lett. **29**, 2837 (2004)
4. P. Maine, G. Mourou, Opt. Lett. **13**, 467 (1988)
5. Q.E. Martinez, IEEE J. Quantum Electron. **23**, 59 (1987)
6. G. Cheriaux, P. Rousseau, F. Salin, J.P. Chambaret, B. Walker, L.F. Dimauro, Opt. Lett. **21**, 414 (1996)
7. E.B. Treacy, IEEE J. Quantum Electron. **5**, 454 (1969)
8. Z. Bor, B. Racz, G. Szabo, M. Hilbert, H.A. Hazim, Opt. Eng. **32**, 2501 (1993)
9. C. Fiorini, C. Sauteret, C. Rouyer, N. Blanchot, S. Seznec, A. Migus, IEEE J. Quantum Electron. **30**, 1662 (1994)
10. G. Pretzler, A. Kasper, K.J. Witte, Appl. Phys. B **70**, 1 (2000)
11. Z. Sacks, G. Mourou, R. Danielius, Opt. Lett. **26**, 462 (2001)
12. K. Osvay, A.P. Kovacs, Z. Heiner, G. Kurdi, J. Klebniczki, M. Csatari, Sel. Areas Commun. **10**, 213 (2004)
13. K. Varju, A.P. Kovacs, G. Kurdi, K. Osvay, Appl. Phys. B **74**, S259 (2002)
14. S. Akturk, M. Kimmel, P. O'Shea, R. Trebino, Opt. Express **11**, 491 (2003)
15. E. Miesak, R. Negres, Appl. Opt. **37**, 8146 (1998)
16. J.L. Collier, C. Hernandez-Gomez, S.J. Hawkes, J. Smith, T.B. Winstone, C.N. Danson, R.J. Clarke, D. Neely, C. Ziener, T. Strange, A.J. Frackiewicz, CLF Annu. Rep. 2002–2003, p. 168